

# An Investigation of Melt Rheology and Thermal Stability of Poly(lactic acid)/ Poly(butylene succinate) Nanocomposites

Amita Bhatia,<sup>1</sup> Rahul K. Gupta,<sup>1</sup> Sati N. Bhattacharya,<sup>1</sup> H. J. Choi<sup>2</sup>

<sup>1</sup>Rheology and Materials Processing Centre, School of Civil, Environmental and Chemical Engineering, RMIT University, Melbourne, Victoria 3001, Australia

<sup>2</sup>Department of Polymer Science and Engineering, Inha University, Incheon 402-751, Korea

Received 3 November 2008; accepted 17 May 2009

DOI 10.1002/app.30933

Published online 16 July 2009 in Wiley InterScience (www.interscience.wiley.com).

**ABSTRACT:** A systematic investigation of the rheological and thermal properties of nanocomposites prepared with poly(lactic acid) (PLA), poly(butylene succinate) (PBS), and organically modified layered silicate was carried out. PLA/PBS/Cloisite 30BX (organically modified MMT) clay nanocomposites were prepared by using simple melt extrusion process. Composition of PLA and PBS polymers were fixed at a ratio of 80 to 20 by wt % for all the nanocomposites. Rheological investigations showed that high clay (> 3 wt %) contents strongly improved the viscoelastic behavior of the nanocomposites. Percolation threshold region was attained between 3 and 5 wt % of clay loadings. With the addition of clay content for these nanocomposites, liquid-like behavior of PLA/PBS blend gradually changed to solid-like behavior as shown by dynamic rheology. Steady shear showed that shear viscosity for the nanocomposites decreased with increasing

shear rates, exhibiting shear-thinning non-Newtonian behavior. At higher clay concentrations, pseudo-plastic behavior was dominant, whereas pure blend showed almost Newtonian behavior. Thermogravimetric analysis revealed that both initial degradation temperature (at a 2% weight loss) and activation energy of thermal decomposition nanocomposite containing 3 wt % of C30BX were superior to those of other nanocomposites as well as to those of PLA/PBS blend. Nanocomposite having 1 wt % of C30BX did not achieve expected level of thermal stability due to the thermal instability of the surfactant present in the organoclay. © 2009 Wiley Periodicals, Inc. *J Appl Polym Sci* 114: 2837–2847, 2009

**Key words:** poly(lactic acid) (PLA); poly(butylene succinate) (PBS); nanocomposites; organoclay; rheological properties; thermal properties

## INTRODUCTION

Recently, studies on biodegradable polymeric materials have become the main research focus for both academic and industrial scientists all over the world. These biodegradable materials can replace nonbiodegradable polymers for the packaging industry, which are causing serious global environmental waste pollution. It is also not entirely justified that for short-lived applications, polymers which are long lived in our environment should be used. Conventional plastics that persist in the environment because of improper disposal are becoming a significantly huge source of environmental pollution and a waste management problem. However, to match the material and physical properties of these biodegradable polymers, developments and investigations on biodegradable nanocomposites is necessary. Silicate layered

polymer nanocomposites demonstrated significant enhancements of a large number of properties including barrier, thermal, mechanical, rheological, flammability resistance, environmental stability, and other physical properties relative to an unmodified or pure polymer resin. These unique improvements in various properties of polymer-silicate nanocomposites are mainly achieved at lower silicate loadings ( $\leq 5$  wt %), which results due to high aspect ratio and high surface area. The high degree of dispersion and the strong interaction between the silicate layers and the polymer matrix provide high interfacial surface-to-volume ratio.<sup>1</sup> Till now various polymer nanocomposites have been developed using layered silicate clay minerals as reinforcing phase because of its easy and abundant availability, low cost, and more importantly environmental friendliness.<sup>2</sup>

It is expected that like other polymer nanocomposites, biodegradable polymer nanocomposites will also demonstrate great enhancements in physical, material, and various properties. Therefore, these biodegradable nanocomposites can definitely become a possible solution for the global environmental

Correspondence to: R. K. Gupta (rahul.gupta@rmit.edu.au).

problem caused by plastic wastes. Various investigations<sup>3,4</sup> have already been done on biodegradable polymers, which are produced from renewable and petroleum resources such as poly(L-lactic acid) (PLA), poly(butylene succinate) (PBS), poly(butylene adipate/terephthalate), poly(ethylene terephthalate/succinate), poly( $\epsilon$ -caprolactone) (PCL) etc. PLA, which is produced from a feedstock of corn rather than petroleum, has been widely used for packaging material. PBS is another biodegradable polymer, which belongs to the family of synthetic polyesters. Since, PLA is produced from the lactide monomer, which comes from lactic acid and is a nontoxic substance readily available in human body; PBS is also a biodegradable polymer and is safe and nontoxic regarding any health related issues. Food contamination can be neglected for PLA and PBS as packaging material. Therefore, it can also be concluded that the nanocomposites produced from these polymers will be self degradable as compared with other commodity polymers.

PLA is a linear thermoplastic polyester having good mechanical properties, thermal plasticity, and good biocompatibility and can be easily fabricated. However, brittleness of PLA, difficulty in processability and due to the ring-opening polymerization of lactide monomer for its production is highly cost demanding process. Due to these two conditions PLA polymer applications has been defected for commercial use. Therefore, compounding of these two biodegradable polymers with clay may improve its processability, enhance its properties and at the same time lower the production cost.

In this study, (PBS) polymer has been chosen to blend with PLA polymer. PBS is chemically synthesized by the polycondensation of 1, 4-butanediol with succinic acid.<sup>5</sup> PBS has high flexibility, excellent impact strength, thermal, and chemical resistance.<sup>6</sup> PBS has excellent processability, so it will also make PLA processability easy. The influence of C30BX and its concentrations on rheological and thermal properties of prepared PLA/PBS/C30BX nanocomposites were examined. PLA/PBS/C30BX nanocomposites having fixed composition of PLA and PBS of 80 and 20 (weight basis) with various clay loadings were prepared. The composition of PLA/PBS blend was fixed on the basis of our preliminary study carried out on various compositions of PLA/PBS blend. Bhatia et al.<sup>7</sup> concluded that 80/20 (PLA/PBS) was the best composition for studying various properties such as morphological, rheological, thermal, and mechanical. Brittleness of PLA was also greatly improved at this blend composition. Full details of this study can be found in our previous publication.<sup>7</sup> Chen and Yoon<sup>8</sup> investigated thermal stability of poly(L-lactide)/poly(butylene succinate)/clay nanocomposites using Cloisite 25A and twice-functional

organoclay (TFC). These authors reported that great improvements in properties of nanocomposites when TFC was used due to the achieved exfoliated morphology and increased interaction between the polyesters and the clay through chemical reaction.

This study is aimed to obtain an extensive understanding of the structure-property relationships and thermal stability of nanocomposites produced by using biodegradable polymers of PLA and PBS by rheological experiments and thermogravimetric analysis, respectively. Rheological property plays an important role in successful processing of polymer-based materials under molten state. Thermal stability through char formation is one of the interesting and widely searched properties displayed by nanocomposites. Organoclay used in this study is the experimental grade, which is expected to provide better dispersion in polymer such as PLA and PBS as compared with the commercially used Cloisite C30B (C30B). Thus, the role of clay has been investigated using rheological and thermal properties.

## EXPERIMENTAL

Following part will provide the brief synopsis of the materials and procedures and/or methods used to produce and investigate various properties of the nanocomposites presented in this article.

### Materials

PLA grade 4032D-biaxially oriented films grade (Nature Works) produced by Cargill Dow LLC was used in this study. And poly(butylene succinate) (PBS) polymer grade G4460, commercially called EnPol, was another biodegradable polyester used to blend with PLA polymer. Both the polymers used in this study have been supplied by Ire Chem. Co., Korea. PLA is a relatively hard biodegradable polymer, but EnPol is soft biodegradable polymer, possessing similar mechanical and manufacturing properties to polyethylene.

Densities of PLA and PBS are 1240 and 1230 kg/m<sup>3</sup>, respectively. PLA has crystalline melting point range between 150 and 170°C, whereas PBS has melting range between 95 and 114.7°C. Melt Index of PBS is 1.8 g/10min (D1238).

Experimental grade of Cloisite 30B organoclay has been used in this study. Cloisite C30B grade is SCPX 3016, however, in this article, this clay has been referred as C30BX. It was supplied by Southern Clay Products (SCP). This clay has basically the same chemical treatment as C30B but has been achieved via a different mechanism.

### Nanocomposites preparation

The pellets of both PLA and PBS were first dried in a vacuum oven at a temperature of 50°C for 48 h to remove moisture before processing through the extruder. Drying of these polymers is very essential as moisture in these polymers helps in hydrolytic chain scission during the processing at high temperature. All the nanocomposites have been prepared by melt compounding the polymers with C30BX clay at 180°C using Brabender twin-screw extruder at 40 rpm. All the nanocomposites have been passed twice through the extruder to achieve better and homogeneous mixing of all the compositions. The composition of binary blends of the PLA/PBS was kept fixed at 80/20 (wt %/wt %) for all the prepared nanocomposites. Nanocomposites of 1, 3, 5, 7, and 10 by wt % of loadings were prepared for the investigations in this study.

All the components were premixed in a bag by tumbling well and were fed simultaneously into the extruder to maintain the overall consistency. The extruded nanocomposites were pelletized and dried again at 50°C in vacuum oven overnight.

### Rheological measurements

Rheological measurements of PLA/PBS blend and its nanocomposites conducted using an Advanced Rheometric Expansion System (ARES-LSII) using 25 mm parallel plates. Tests were performed at 175°C under a nitrogen atmosphere to avoid any degradation. All samples were dried in a vacuum oven before the test and a fresh sample was loaded for each type of rheological test. Disk shaped samples of 25 mm were stamped out from the 2 mm thick plaque made by using compression molding machine at 200°C and pressure of 40 kN for 5 min.

First of all, dynamic strain sweep tests were carried out to confirm the linearity of viscoelastic region up to 100% strain at 10 rad/s frequency. All measurements for dynamic frequency sweep tests were performed over a frequency range of 0.1 to 100 rad/s and steady shear rate sweeps tests were done using steady shear mode over a shear rate range of 0.1–100 s<sup>-1</sup> at 10% strain.

### Thermal properties

Thermal properties of PLA/PBS/C30BX nanocomposites were examined using a thermogravimetric analyzer (TGA) (Q50 thermogravimetric analyzer V6.4, TA Instruments, Delaware). Samples of ~20–25 mg masses were heated from 25 to 600°C at a heating rate of 25°C/min under nitrogen atmosphere. Samples were placed in a Platinum pan. During the test, balance gas used was nitrogen with flow rate of 10

mL/min, and sample gas (nitrogen) with flow rate of 90 mL/min.

## RESULTS AND DISCUSSION

### Rheological properties

Preliminary studies were conducted on PLA/PBS blend and their nanocomposites to ensure that the dynamic properties were measured in the linear viscoelastic region. Dynamic strain sweep test is very much essential before performing dynamic frequency sweep test to ensure the linear viscoelastic region of the material. Linear viscoelastic region tells that within this region the configuration of the macromolecules would remain unperturbed by the flow history.<sup>9</sup> It means that microstructure of the material would not be affected by shear alignment during the experiment. Dynamic strain sweep tests were conducted at 175°C temperature for PLA/PBS (80/20) blend and its nanocomposites having various amounts of C30BX at a constant frequency of 10 rad/s (Fig. 1). The linear region of each curve depicts linear viscoelastic behavior of that particular material.

All the nanocomposites except 1 wt % of clay exhibited highly pronounced nonlinear behavior, where onset of the  $G'$  drop occurred around critical strain of 2.5%. It was also observed that as the concentration of C30BX was increased the material remained independent of decreased strain%. The limit of linearity of viscoelastic region tended toward low strains amplitudes (%) at higher clay concentrations. C30BX of 1 wt % showed linear viscoelastic region up to 40% strain. Due to the interaction between the polymer and the clay particles, nanocomposites exhibited solid-like behavior. In the linear region, the mesostructure of the material remains in the quiescent state and the imposed deformation or strain is absorbed by the material. The

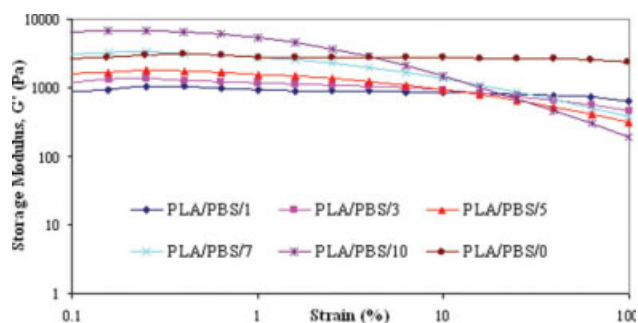


**Figure 1** Evaluation of the linear viscoelastic response of PLA/PBS (80/20) blend and PLA/PBS/C30BX nanocomposites having various loadings of clay at a constant frequency of 10 rad/s and 175°C. [Color figure can be viewed in the online issue, which is available at [www.interscience.wiley.com](http://www.interscience.wiley.com).]

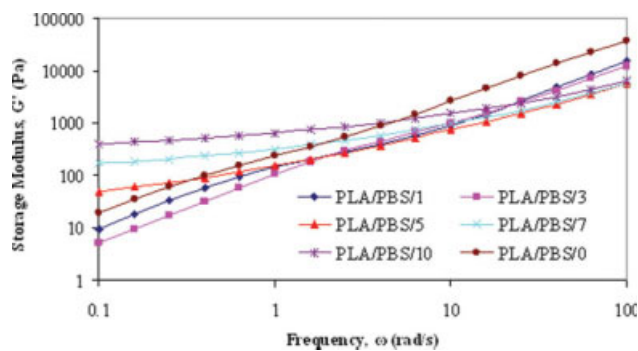


**Figure 2** Storage modulus,  $G'$  versus frequency at 175°C of PLA/PBS (80/20) blend and PLA/PBS/C30BX nanocomposites with various clay loadings. [Color figure can be viewed in the online issue, which is available at [www.interscience.wiley.com](http://www.interscience.wiley.com).]

strain applied is not high enough to unrest its equilibrium state. The critical strain amplitude marks the onset of alignment of silicate layers at lower strain amplitudes. During high shear, mesostructure of the material began to align in the direction of the shear flow. Krishnamoorti et al.<sup>10</sup> described these alignments as similar to that observed in crystalline polymers and block copolymers.

The subsequent dynamic frequency sweeps tests were conducted at strain amplitudes within the linear viscoelastic region. Figures 2 and 3 show the response of frequency on the storage modulus ( $G'$ ) and loss modulus ( $G''$ ) for PLA/PBS blend and its nanocomposites. Considering storage modulus and loss modulus of PLA/PBS blend alone, this blend showed similar behavior as neat PLA and PBS as shown in our earlier investigation (Bhatia et al.<sup>7</sup>).

Both storage and loss moduli of PLA/PBS (80/20 by wt %) blend and its nanocomposites increased monotonically at all frequencies and showed terminal behavior at lower frequencies for high clay concentrations nanocomposites. The reason for the terminal region in the nanocomposites at high concentration of clay may be due to the intercalation of the clay particles. It was interesting to note that nanocomposites with 1 and 3 wt % of clay behaved similar to that of PLA/PBS blend. At low frequencies, there was a decrease in  $G'$  (storage modulus) when the concentration of C30BX was increased from 0 to 3 wt %, whereas at higher frequencies storage modulus of 1 and 3 wt % nanocomposites approached similar values. Storage modulus of PLA/PBS blend was always higher as compared with 1 and 3 wt % of nanocomposites over the entire frequency range (0.1–100 rad/s) investigated. Also, blend showed higher storage modulus and loss modulus as compared with all the nanocomposites at higher frequencies. Nanocomposites of higher clay concentration that is nanocomposites having 5,

7, and 10 wt % of C30BX demonstrated increase in  $G'$  especially at low frequencies, whereas at higher frequency regions,  $G'$  all these nanocomposites were quite similar. Increase in silicate concentration increased the solid-like or elastic nature of the nanocomposites. At high frequencies, the viscoelastic behavior of these three nanocomposites was quite similar except only a small systematic increase in  $G'$  with C30BX loading was noticed. This indicates that the observed chain relaxation modes are almost unaffected by the presence of the layered silicate particles (Figs. 2 and 3). However, at the low frequency region, both dynamic moduli exhibited weak frequency dependence in nanocomposites with higher concentrations of C30BX. Due to the present of big coagulated clay particles in the high clay nanocomposites as compared with the low clay nanocomposites, the drastic change of slope at terminal region (low frequency region) can be noticed. For nanocomposites having 7 and 10 wt % of C30BX loadings,  $G'$  became nearly independent of frequency. Nanocomposites having 5, 7, and 10 wt % C30BX demonstrated remarkably strong viscoelastic improvements. The rheological behavior of the intercalated nanocomposites depends both on the intercalation of the polymer chains and on the alignment of the silicate layers.<sup>11</sup> WAXD and TEM results discussed in our previous journal<sup>12</sup> indicated intercalation structure for 5, 7, and 10 wt % of nanocomposites. Whereas poly(butylene succinate) nanocomposites revealed the formation of intercalated nanocompositions, regardless of the silicate loading.<sup>13</sup> Interlayer d-spacing (corresponding to  $d_{001}$ , diffraction peaks) of clay and nanocomposites calculated by using Bragg's law can be seen in Table I. Micrographic images of the blend and their nanocomposites are shown in Figure 4. With the addition

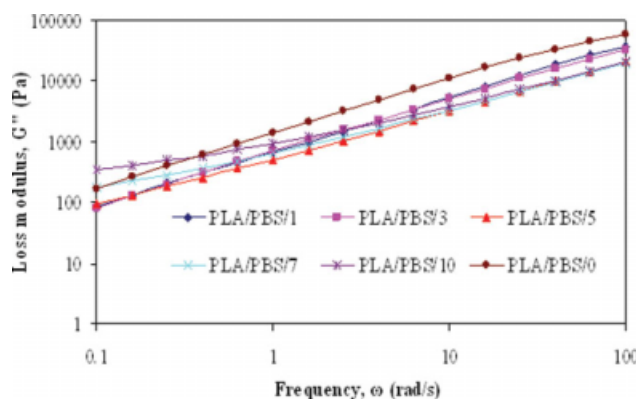


**Figure 3** Loss modulus,  $G''$  versus frequency at 175°C of PLA/PBS (80/20) blend and PLA/PBS/C30BX nanocomposites with various clay loadings. [Color figure can be viewed in the online issue, which is available at [www.interscience.wiley.com](http://www.interscience.wiley.com).]

**TABLE I**  
**Interlayer Spacing as Determined by WAXD Analysis**  
**(Bragg's law). [Number in the Bracket indicates**  
**loadings of clay]**

Sample	Diffraction angle ( $2\theta$ )	Interlayer spacing ( $\text{\AA}$ )
C30BX clay	$4.96^\circ$	17.8
PLA/PBS/C30BX (1 wt %)	–	exfoliated
PLA/PBS/C30BX (3 wt %)	–	exfoliated
PLA/PBS/C30BX (5 wt %)	$2^\circ$	44.12
PLA/PBS/C30BX (7 wt %)	$2.2^\circ$	40.10
PLA/PBS/C30BX (10 wt %)	$2.3^\circ$	38.36

of 1 wt % of C30BX in PLA/PBS (80/20) blend, particle size reduced significantly. The excessive surfactant used to modify the clay and the increased viscosity may be considered as the reasons behind the reduction of the domain size.

Although, WAXD pattern of nanocomposite having 3 wt % of clay showed featureless diffraction, which meant exfoliated morphology, TEM image [Fig. 5(c)] showed delaminated and stacked structure of the silicate layers with higher magnification. More precisely, 3 wt % of C30BX exhibited mixed intercalated/exfoliated morphologies or disordered intercalated structure of stacked silicates. Therefore, nanocomposites with 1 and 3 wt % of C30BX are expected to achieve greater enhancement in mechanical, rheological, thermal, and especially barrier properties, some of them will be discussed in the upcoming sections.

Big, clear and flocculated silicate layer tactoids can be seen in 5, 7, and 10 wt % of nanocomposites. These tactoids are of average size of 40 nm. It can be seen that increasing the clay concentration, the thickness of tactoids increased. However, these tactoids

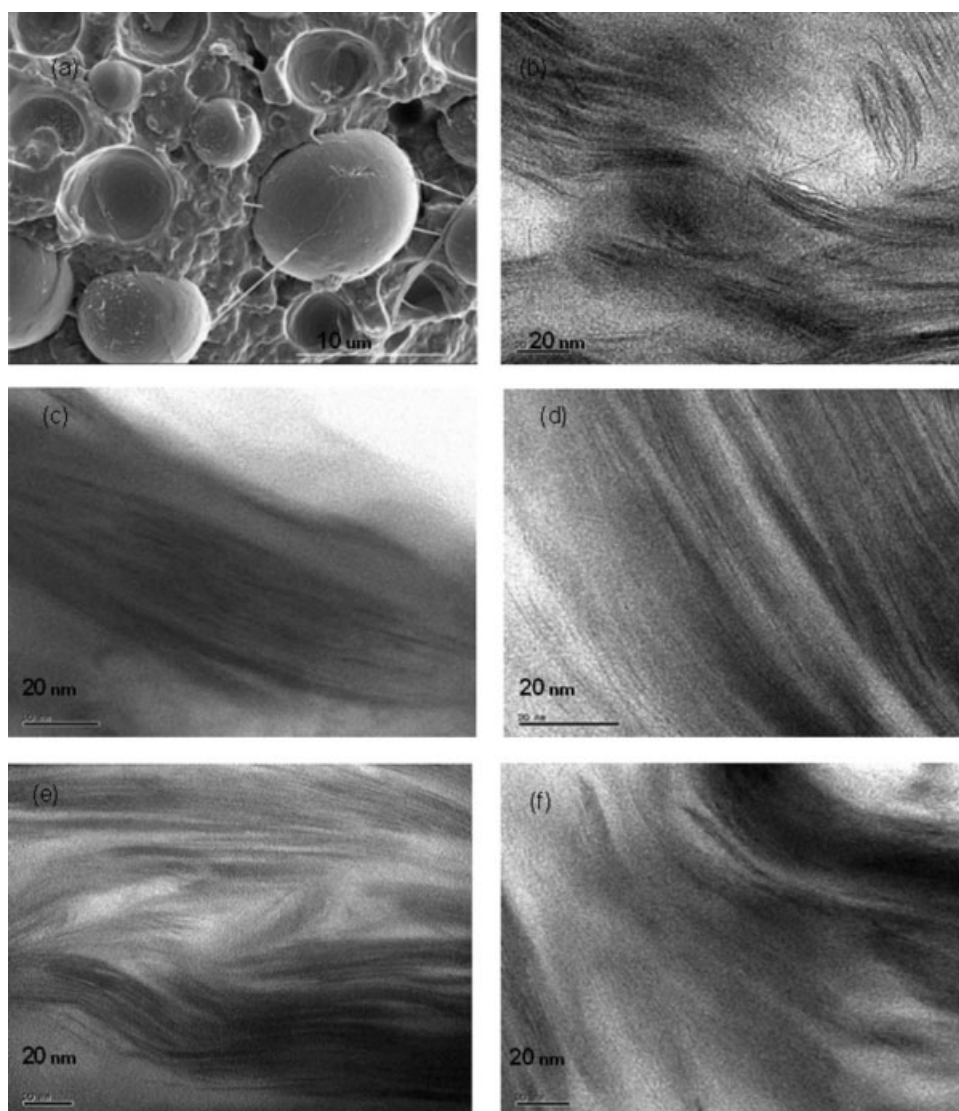


**Figure 4** TEM images of PLA/PBS/Cloisite 30BX nanocomposites containing: (a) 0 wt %, (b) 1 wt %, (c) 3 wt %, (d) 5 wt %, (e) 7 wt %, and (f) 10 wt % clay. PLA/PBS ratio is 80/20 by wt % for all the nanocomposites.

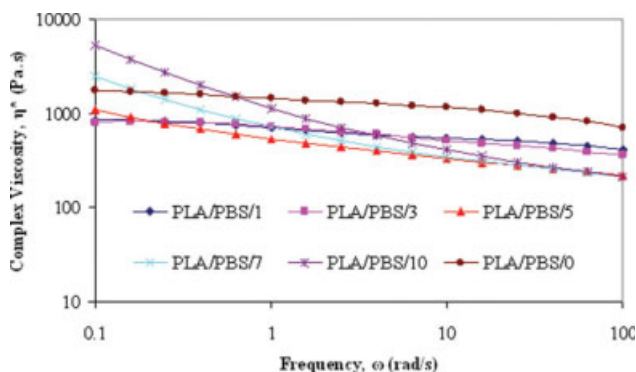


**Figure 5** Complex viscosity, ( $\eta^*$ ) versus frequency at 175°C of PLA/PBS (80/20) blend and PLA/PBS/C30BX nanocomposites with various clay loadings. [Color figure can be viewed in the online issue, which is available at [www.interscience.wiley.com](http://www.interscience.wiley.com).]

themselves gain some degree of disorderness. TEM images clearly demonstrated stacked and intercalated silicate layers were nicely dispersed in the PLA and PBS matrices. WAXD analysis also confirmed the formation of intercalated nanocomposites.

Similarly,  $G''$  (loss modulus) also showed improvements Figure 3.  $G''$  is viscoelastic parameter that indicates the viscous or liquid-like behavior of the material, and it gives information mainly on the viscous or energy dissipation during flow.<sup>14</sup> Loss modulus for the blend and its nanocomposites also increased monotonically over the frequency range investigated in this study. At high frequency region, the anisotropic silicate platelets or stacks of platelets get aligned in the direction of the flow, therefore, less increase in  $G''$  was observed. The limited contribution at high frequency region was observed for both the dynamic moduli for all the nanocomposites. For PLA/PBS nanocomposites with C30BX loading in excess of 3 wt %, the liquid-like behavior observed in neat PLA/PBS blend gradually changed to pseudo-solid-like behavior. Nanocomposites containing 1 and 3 wt % of C30BX showed larger enhancements from low to high frequency regions. High clay concentrations nanocomposites also demonstrated enhancements but have lesser slopes. The reason may be high content of silicate layers makes alignment easy and quickly during high frequencies.

Figure 6 shows the slope of  $G'$  at low frequencies (0.1–1 rad/s) versus clay concentration (wt %) for PLA/PBS/C30BX nanocomposites. The slope,  $\alpha$ , as seen from Figure 6 decreased from clay loading 1 wt % to 3 wt %, then remained stable to 5 wt % and then increased sharply for 10 wt % of clay loading in nanocomposites. This change in slope marks the percolation threshold value (critical loading) of C30BX in PLA/PBS nanocomposites. Slopes of 3 and 5 wt % of nanocomposites were almost similar. In this work, only limited nanocomposites were pre-

pared on which rheological studies were performed. May be abrupt change in slope could be seen in 4 wt % of C30BX nanocomposite. Therefore, percolation threshold region of PLA/PBS/C30BX nanocomposites in this research work comes out in between 3 and 5 wt % of clay. XRD and TEM results also concluded that up to 3 wt % of clay, nanocomposite have mixed morphology of exfoliated and intercalated nanostructure but after that exfoliation started to decrease, predominantly intercalated and latter on agglomerates were formed.<sup>12</sup> For other polymers nanocomposites like polypropylene nanocomposites, threshold value is normally 2.5 wt % of clay, where as in this case (PLA/PBS/C30BX nanocomposites) threshold value ranged between 3 wt % and 5 wt %. This is because of the polar nature of both the polymers (PLA and PBS) used to prepare PLA/PBS/C30BX nanocomposites.

The threshold value corresponds to the formation of three-dimensional network structure whereby silicate layers act as physical cross-linkers. Ayyer and Leonov<sup>15</sup> attributed percolation threshold depends upon the number of silicate platelets per tactoid and the aspect ratio of the platelets. At low filler fractions, the particles are percolated within the polymer matrix and as soon as the filler fraction reached its maximum packing fraction, the polymer got entrap within the interstices of the filler network. Mela and Alberola<sup>16</sup> corresponded this maximum packing fraction to the percolation threshold. Increase in silicate loading increases the packing density of silicates in the polymer matrix. Packing density increases much when the clay tactoids or agglomerates are well dispersed and distributed within the matrix and thus increase the surface area of contact between the polymer matrix and silicate layers.<sup>17</sup> Yurekli et al.<sup>18</sup> worked on carbon-black-filler elastomers and noted that pseudo-solid-like behavior observed in storage modulus was due to the evolution of network structures.

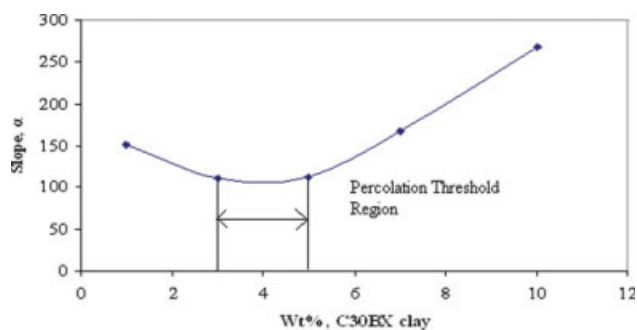


**Figure 6** Slope ( $\alpha$ ) of  $G'$  at low frequency as a function of C30BX clay loading (wt %) for PLA/PBS/C30BX nanocomposites. [Color figure can be viewed in the online issue, which is available at [www.interscience.wiley.com](http://www.interscience.wiley.com).]

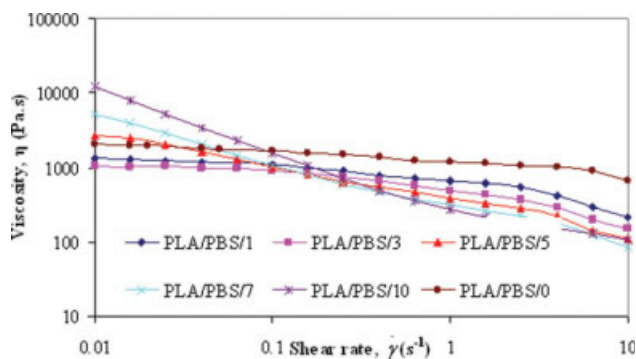


**Figure 7** Steady shear viscosity ( $\eta$ ) versus shear rate ( $\dot{\gamma}$ ) at 175°C of PLA/PBS (80/20) blend and PLA/PBS/C30BX nanocomposites with various clay loadings. [Color figure can be viewed in the online issue, which is available at [www.interscience.wiley.com](http://www.interscience.wiley.com).]

Complex viscosities ( $\eta^*$ ) of PLA/PBS blend and its nanocomposites having various loadings of C30BX are shown in Figure 5. Nanocomposites having 1 and 3 wt % of clay followed the same path of PLA/PBS blend; however, PLA/PBS blend has higher viscosity than these two nanocomposites. The blend and nanocomposites with less concentration of clay exhibited almost Newtonian behavior in the investigated frequency range. While, nanocomposites of 5, 7, and 10 wt % of clay showed strong shear-thinning tendency over the frequency range investigated in this work. Evidently, as the filler concentration was increased, the complex viscosity increased mainly at low frequencies only. At high frequencies, complex viscosities coincided with each other. At high clay loadings, due to the alignment of the silicate layers in the direction of the shear, shear-thinning characteristic was clearly seen. Little effect of C30BX addition was observed at high frequencies, where the relaxation mechanism was mainly dominated by that of the polymer matrices, whereas at low frequencies, the relaxation was due to the particle-particle interactions inside the percolation network of the silicate layers.<sup>19</sup> Overall, complex viscosity behavior of the nanocomposites was similar to that of storage moduli (Fig. 2), where higher concentrations of clay content demonstrated gradual change from the liquid-like behavior observed in neat PLA/PBS blend to pseudo-solid-like behavior in nanocomposites.

The dependence of steady shear viscosity ( $\eta$ ) on shear rate ( $\dot{\gamma}$ ) as measured by constant rate steady shear measurements for PLA/PBS blend and its nanocomposite have been shown in Figure 7. Shear viscosity of all the nanocomposites decreased with increase in shear rate, exhibiting non-Newtonian shear-thinning behavior down to the lowest shear rates probed. With the increase of C30BX content in the nanocomposites, the pseudo-plastic behavior is

becoming more dominant. According to Choi et al.<sup>20</sup> the shear-thinning nature of these nanocomposites means that they can be easily melt processed. Shear viscosity of PLA/PBS blend almost remained constant over the investigated range of shear rates exhibiting Newtonian characterization. During the melt process method in twin-screw extruder, the nanocomposites were much easier to handle especially nanocomposites with high concentration of C30BX clay loadings as compared with PLA/PBS blend.

Nanocomposites having 1 and 3 wt % of C30BX also showed Newtonian behavior but only at low shear rates followed by continuous shear-thinning behavior. In the case of nanocomposites having 5, 7, and 10 wt % of clay, the shear viscosity increased with clay loadings with increase in shear rates. The increase in viscosity is a result of increased interactions between the silicate layers and PLA and PBS polymer chains.<sup>20</sup> They also exhibited shear-thinning behavior, particularly at higher shear rates. At high shear rates, the viscosity of the nanocomposites was nearly independent of the filler loading, suggesting that the silicate layers and their tactoids contribute negligibly to the overall viscosity because of their ability to be aligned by the application of shear flow.<sup>10</sup> Nanocomposites with highest clay loadings exhibited a divergence of the viscosity consistent due to the formation of a percolated filler network structure.<sup>21</sup> These nanocomposites (7 and 10 wt % of C30BX clay) did not show any sign of zero-shear plateau which may be due to the presence of three-dimensional network structure. Also, viscosities of nanocomposites containing higher clay loadings (5, 7, and 10 wt %) increased with the addition of clay at low and intermediate shear rate ranges, and then decreased after crossover point at low shear rates. Viscosities of PLA/PBS blend and nanocomposites with 1 and 3 wt % of C30BX were lower than nanocomposites having 5, 7, and 10 wt % of clay at low shear rate ranges, and then it increased at high shear rate ranges. Also, at lower shear rates ( $<0.1 \text{ s}^{-1}$ ); the viscosity increase was monotonically higher with increase in C30BX content in PLA/PBS polymer blend, whereas at high shear rate ranges viscosity change was negligible.

From the observed enhancement in shear-thinning behavior at low shear rates in high clay content nanocomposites, it can be concluded that this could be resulted from the polymer imprisonment between clay particles and layers, by which a larger effective strain rate may be experienced.<sup>22,23</sup> Viscosities of many filled systems are generally higher than their neat polymer due to the enhanced energy dissipation in the presence of solid particles. That is why in low concentration regimes the viscosities are quite similar to the neat polymer because of the little

interparticle interactions as demonstrated by 1 and 3 wt % of PLA/PBS/C30BX nanocomposites in this work.

### Thermal characterization

Thermal stability of the nanocomposites was evaluated by TGA, where the weight loss due to the volatilization of degradation by-products was monitored as a function of temperature. Figure 8 shows thermograms of thermal stability of polymer blend PLA/PBS, (80/20) and their nanocomposites when filled with different loadings of C30BX.

The onset initial degradation temperature ( $T_{iD}$ ) (at 2% weight loss) was measured from the intersection of the tangent of the initial point and the inflection point and is reported in Table II. It is clear that only 3 wt % of nanocomposite showed highest thermal stability to that of the PLA/PBS blend and their nanocomposites. Thermal stability of PLA/PBS blend decreased with the incorporation of 1 wt % of clay, however, thermal stability of nanocomposites get improved with the addition of more clay. It meant that thermal insulation happened in this system at higher temperatures with the nanocomposites having 3 or more than 3 wt % of C30BX. Initial degradation temperature of the nanocomposites started to decrease with the addition of C30BX beyond 3 wt %, however, their onset initial degradation temperatures were higher than PLA/PBS blend. Nanocomposite having 3 wt % of clay is considered as the optimum value for the enhancement of the thermal stability in PLA/PBS/C30BX nanocomposites. This optimum value or threshold value is relevant to the results obtained in rheological properties as discussed previously and mechanical and gas barrier measurements of these nanocomposites, details of which are given in prior publications.<sup>12</sup> The systematic decrease in thermal stability of PLA/PBS/

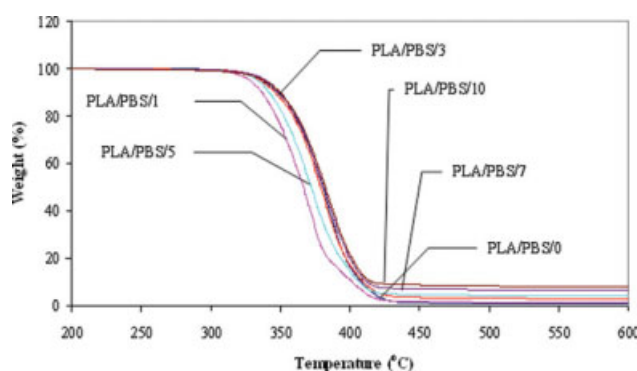


**Figure 8** TGA curves of PLA/PBS blend and PLA/PBS/C30BX nanocomposites with various clay loadings. PLA/PBS ratio is fixed by wt % (80/20) for all the nanocomposites. [Color figure can be viewed in the online issue, which is available at [www.interscience.wiley.com](http://www.interscience.wiley.com).]

**TABLE II**  
Thermal Stability Parameters of the PLA/PBS (80/20) Blend and PLA/PBS/C30BX Nanocomposites Having Various Clay Loadings. [Number in the Bracket Indicates Loadings of Clay.]

Nanocomposites (PLA/PBS/C30BX)	Initial degradation temperature, $T_{iD}$ (°C)	Activation energy of decomposition, $E_t$ (kJ/mol)
PLA/PBS/C30BX (0 wt %)	338	2109
PLA/PBS/C30BX (0 wt %)	335	1980
PLA/PBS/C30BX (0 wt %)	355	3151
PLA/PBS/C30BX (0 wt %)	340	1841
PLA/PBS/C30BX (0 wt %)	350	1991
PLA/PBS/C30BX (0 wt %)	348	1990

C30BX nanocomposites after 3 wt % of C30BX loading may be due to the presence of excess amount of hydroxyl groups in the organic modifier that provided a supply of excess oxygen.<sup>19</sup> Another reason may be the poor dispersion or the accumulation of clay particles between the interface at higher concentration of C30BX being suggested by the WAXD and TEM, and MDSC results, respectively.<sup>12</sup>

Various studies have been published for other nonbiodegradable nanocomposites using various types of organo-modified montmorillonite silicate layers with matrices such as nylon-6,<sup>24</sup> polystyrene,<sup>25</sup> ethylene-vinyl acetate copolymer<sup>26</sup> or PCL.<sup>27</sup> All these studies showed enhancement in thermal stability with the addition of organoclay. Zanetti et al.<sup>26</sup> attributed the improvement of thermal stability of the nanocomposites to the shielding effect of the clay layers present in the polymer matrices. Small molecules generated during the thermal degradation process have to take a long way around the clay layers to pass through because the layers of organo-modified silicate are impermeable. In this research work, it was noted that PLA/PBS/C30BX nanocomposite having 1 wt % of clay degraded at a little faster rate as compared with the pure polymer blend. This may be due to the excess organic modifier present on the clay surface. Another reason for this result may be due to the thermal instability of the surfactant, as alkyl ammonium modifiers are known to undergo Hoffman degradation around 200°C.<sup>19</sup>

It is interesting to note that after 375°C, 7 and 10 wt % nanocomposites degraded at much slower rate compared with that of PLA/PBS blend; however, the degradation rates of 1 and 5 wt % of nanocomposite were almost similar to the blend. This was most unexpected observation in this work because one of the property enhancement expected upon the formation of nanocomposites was the retardation of the thermal degradation which directly related to the amount of clay loading.<sup>28</sup> Degradation of 7 and



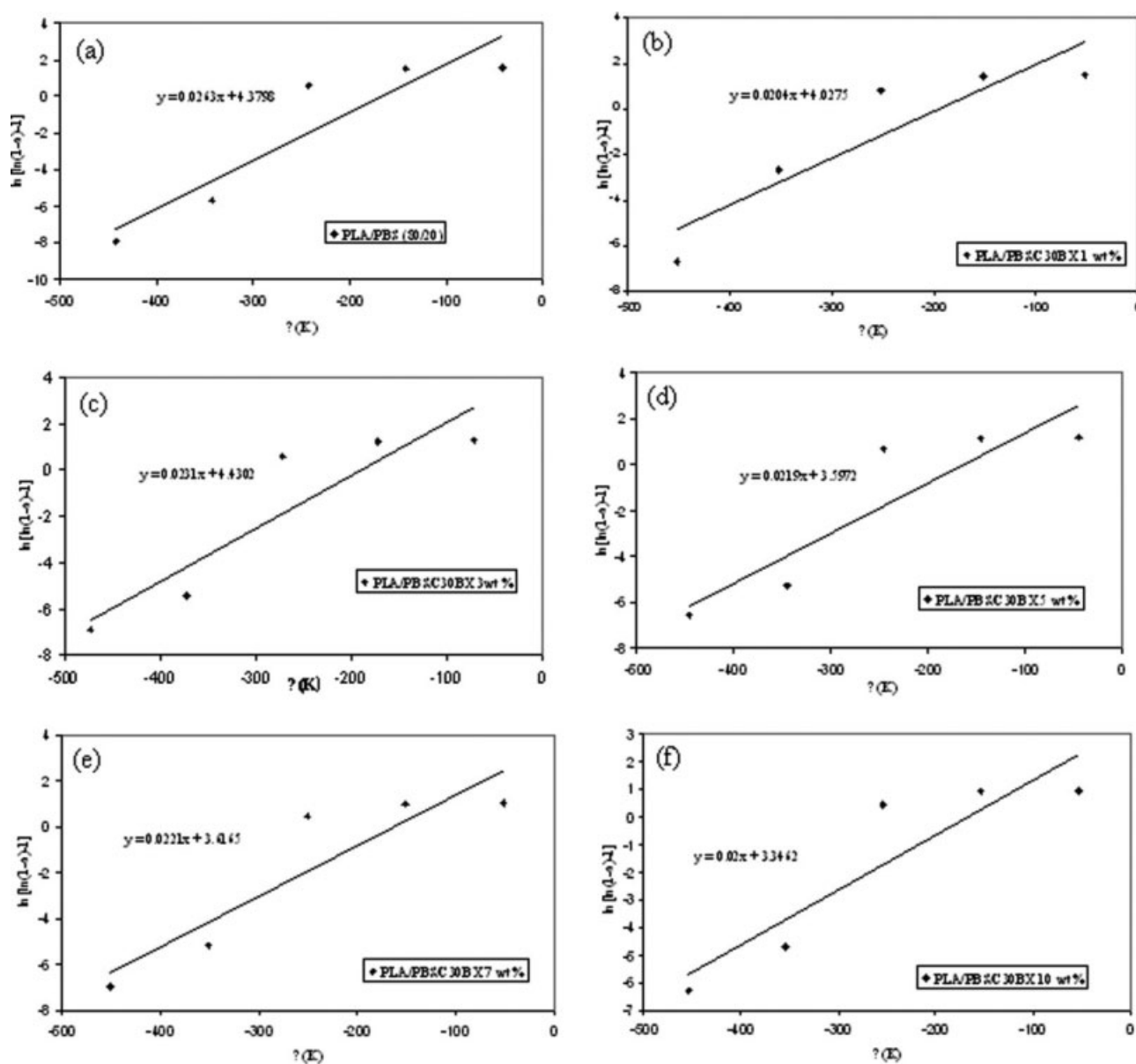


**Figure 9** Plot of  $\ln[\ln(1-\alpha)^{-1}]$  vs.  $\theta$  of PLA/PBS/C30BX nanocomposites (a-f) having 1, 3, 5, 7, and 10 wt % of C30BX for determination of the decomposition activation energy. Straight line is the best linear fit of the data points.

10 wt % nanocomposites became slow as there was only inorganic aluminosilicate left in the system at high temperature and the amount of the inorganic residue left linearly increased with the wt % of C30BX originally incorporated into PLA/PBS blend. Paul et al.<sup>29</sup> also observed a slight decrease in thermal stability at a high loading of clay in plasticized PLA polymer. The protective silicate layer seemed to be less effective at higher concentrations of C30BX in PLA/PBS/C30BX nanocomposites than that obtained from the nanocomposites having lower concentration of clay. This was perhaps related to the poor dispersion of C30BX in PLA and PBS polymers sample at high clay concentrations.

Activation energy for decomposition,  $E_t$  of PLA/PBS blend and PLA/PBS/C30BX nanocomposites were calculated from the TGA curves by integral method proposed by Horowitz and Metzger<sup>30</sup> according to the eq. (1).

$$\ln\left[\ln\left(\frac{1}{1-\alpha}\right)\right] = \frac{E_t\theta}{RT_{\max}^2} \quad (1)$$

where  $\alpha$  is the decomposed fraction,  $E_t$  is the activation energy of decomposition,  $T_{\max}$  is the temperature at maximum rate of weight loss,  $\theta$  is  $(T - T_{\max})$ , and  $R$  is the universal gas constant.

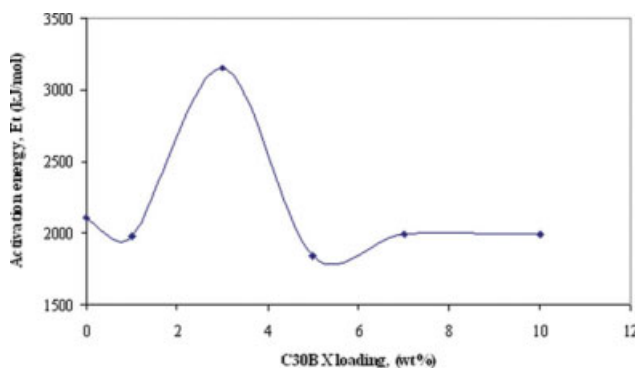


**Figure 10** Effects of C30BX loading on activation energy calculated by using eq. (1) using Horowitz-Metzger method. [Color figure can be viewed in the online issue, which is available at [www.interscience.wiley.com](http://www.interscience.wiley.com).]

Various plots between  $\ln[\ln(1-\alpha)^{-1}]$  vs.  $\theta$  have been shown in Figure 9. The activation energy for decomposition can be determined using the slope of the straight line from eq. (1). The calculated values of activation energy for decomposition are summarized in Table II. The determined activation energy as a function of the C30BX loading in PLA/PBS blend is shown in Figure 10. The activation energy of the nanocomposites reached a maximum value of 3151 (kJ/mol) when the concentration of C30BX was 3 wt % in PLA/PBS binary system. The initial degradation temperature and the activation energy for decomposition seemed to be quite related to each other. Both the initial degradation temperature and the activation energy of decomposition of PLA/PBS/C30BX nanocomposite seemed to provide similar conclusion that was obtained from morphological,<sup>12</sup> rheological, mechanical<sup>12</sup> and thermal properties studied on these nanocomposites.

Guo et al.<sup>31</sup> and Chen and Yoon<sup>8</sup> also reported that the activation energy is dependent on the clay loading. As concentration of clay increased, the activation energy also increased. Exfoliated silicate layers nanocomposites are considered to be thermally more stable than those with intercalated silicate layers.<sup>8,31</sup> Nanocomposites in this research work did not show much enhancement in comparison to PLA/PBS blend for thermal stability and activation energy of the nanocomposites except 3 wt % of C30BX. Activation energy of PLA/PBS blend was higher in comparison to all the PLA/PBS/C30BX nanocomposites except 3 wt % of C30BX. The retardant effects of the exfoliated platelet to heat and oxygen in polymer is strengthened when the OMMT loading is less but as OMMT loading increases further, the nanocomposites develop an exfoliated/intercalated structure.<sup>31</sup> Tactoids are less effective in blocking heat and oxygen than exfoliated platelets. As a consequence, the activation energy decreases when the organoclay loading increased. PLA/PBS/C30BX (3 wt %) nanocompo-

sites showed highest activation energy even though 1 wt % of C30BX nanocomposite was having good morphology. This trend is something unusual from the normal nanocomposites. This may be due to the effective char yield formation on the residual polymer at 3 wt % of C30BX. 5, 7 and 10 wt % of C30BX nanocomposites showed lower activation energy as expected due to the intercalated structure and tactoids formation of clay.

## CONCLUSIONS

Various rheological and thermal data on PLA/PBS/C30BX nanocomposites with different loadings of clay have been studied and correlated with the nanostructure of the nanocomposites obtained during the melt process method. During the dynamic oscillatory tests, it was concluded that both storage and loss moduli increased with frequency. There was insignificant much change in viscoelastic behavior at low clay content (i.e., 1 wt % and 3 wt %), whereas high clay content strongly improved the viscoelastic behavior of the nanocomposites. In the low frequency region, nanocomposites of high clay content attained terminal region. With the increase in concentration of C30BX liquid-like behavior of PLA/PBS blend gradually changed to solid-like. The percolation threshold region for PLA/PBS/C30BX nanocomposites was deemed to lie between 3 and 5 wt % of clay loadings. That may be the reason for all the investigated parameters being changed abruptly with 3 wt % of clay loadings. Steady shear rheology showed that shear viscosity for the nanocomposites decreased with shear rate, exhibiting shear-thinning behavior. At higher clay concentrations pseudo-plastic behavior was dominant, while pure blend showed almost Newtonian behavior. At higher shear rates, shear viscosities of 5, 7, and 10 wt % nanocomposites approached each other suggesting that the silicate layers and their tactoids contribute negligibly to the overall viscosities due to the alignment in the flow direction by shear flow. Thermogravimetric analysis showed that nanocomposite containing 3 wt % of C30BX demonstrated highest thermal stability compared with other nanocomposites. Nanocomposite having 1 wt % of C30BX did not achieve expected level of thermal stability due to the thermal instability of the surfactant present in the organoclay.

## References

1. Giannelis, E. P. *Adv Mater* 1996, 8, 29.
2. Grim, R. E. *Clay Mineralogy*; McGraw-Hill: New York, 1953.
3. Garlotta, D. *J Polym Environ* 2001, 9, 63.
4. Fujimaki, T. *Polym Degrad Stab* 1998, 59, 209.
5. Bhari, K.; Mitomo, H.; Enjoji, T.; Yoshii, F.; Makuuchi, K. *Polym Degrad Stab* 1998, 62, 551.
6. Doi, Y.; Fukuda, K. *Stud Polym Sci* 1994, 12, 627.

7. Bhatia, A.; Gupta, R. K.; Bhattacharya, S. N.; Choi, H. J. *Korea-Australia Rheol J* 2007, 19, 125.
8. Chen, G. X.; Yoon, J. S. *Polym Degrad Stab* 2005, 88, 206.
9. Carreau, P. J.; Degee, D. C. R.; Chhabra, R. P. *Rheology of Polymeric Systems: Principles and Applications* Munich; Hanser Publishers: New York, 1997.
10. Krishnamoorti, R.; Ren, J.; Silva, A. S. *J Chem Phys* 2001, 114, 4968.
11. Lim, Y. T.; Park, O. O. *Macromol Rapid Commun* 2000, 21, 231.
12. Bhatia, A.; Gupta, R. K.; Bhattacharya, S. N.; Choi, H. J. *Int Polym Process* 21 July 2008, IPP 2214.
13. Sinharay, S.; Okamoto, K.; Okamoto, M. *J Appl Polym Sci* 2006, 102, 777.
14. Greene, J. P.; Wilkes, J. O. *Polym Eng Sci* 1995, 35, 1670.
15. Ayyer, R. K.; Leonov, A. I. *Rheologica Acta* 2004, 43, 283.
16. Mele, P.; Alberola, N. D. *Compos Sci Technol* 1996, 56, 849.
17. Prasad, R. Thesis in School of Civil and Chemical Engineering, Royal Melbourne Institute of Technology, Melbourne, 2005.
18. Yurekli, K.; Krishnamoorti, R.; Tse, M. F.; McElrath, K. O.; Tsou, A. H.; Wang, H. C. *J Polym Science Part B Polym Phys* 2001, 39, 256.
19. Sinharay, S.; Bousmina, M.; Okamoto, K. *Macromol Mater Eng* 2005, 290, 759.
20. Choi, H. J.; Kim, S. G.; Hyun, Y. H.; Jhon, M. S. *Macromol Rapid Commun* 2001, 22, 320.
21. Ren, J.; Silva, A. S.; Krishnamoorti, R. *Macromolecules* 2000, 33, 3739.
22. Granick, S. *Mater Res Soc Bull* 1996, 21.
23. Subbotin, A.; Semenov, A.; Manias, E.; Hadziioannou, G.; Ten Brinke, G. *Macromolecules* 1995, 28, 1511.
24. Liu, L.; Qi, Z.; Zhu, X. *J Appl Polym Sci* 1999, 71, 1133.
25. Zhu, J.; Wilkie, C. A. *Polym Int* 2000, 49, 1158.
26. Zanetti, M.; Camino, G.; Mulhaupt, R. *Polym Degrad Stab* 2001, 74, 413.
27. Lepoittevin, B.; Pantoustier, N.; Devalckenaere, M.; Alexandre, M.; Kubies, D.; Calberg, C.; Jerome, R.; Dubois, P. *Macromolecules* 2002, 35, 8385.
28. Gilman, J. W. *Appl Clay Sci* 1999, 15, 31.
29. Paul, M. A.; Alexandre, M.; Degee, P.; Henrist, C.; Rulmont, A.; Dubois, P. *Polymer* 2003, 44, 443.
30. Horowitz, H. H.; Metzger, G. *Anal Chem* 1963, 35, 1464.
31. Guo, B.; Jia, D.; Cai, C. *Eur Polym J* 2004, 40, 1743.